ABUNDANCES AND CHARGE STATES OF PARTICLES IN THE SOLAR WIND

Peter Bochsler[1]
Space Physics Group
Department of Physics
University of Maryland
College Park

Abstract. The Sun is the only star from which matter can be collected in order to investigate its elemental and isotopic composition. Solar elemental abundances provide the most important benchmark for the chemical evolution of the galaxy. They can be derived from photospheric observations, from in situ investigations of the solar wind, and from solar energetic particles. Solar isotopic abundances provide an important reference for the galactic evolution and if available with sufficient precision, also for the chemical and physical evolution of the solar system. The abundances of isotopes in the solar atmosphere can only be inferred from in situ observations of solar particles. This review makes an attempt to summarize current knowledge about the composition of the solar wind and shows how the elemental, isotopic, and charge state composition of solar wind particles is shaped as the solar corona expands throughout the heliosphere.

1. INTRODUCTION

For a typical physicist the occupation with natural abundances has some negative connotations. Dealing with abundances implies bookkeeping, filling in tables, maintaining inventories, dull and uninspiring things which involve dead matter and not much action. The following review is not intended to convert disbelievers. These introductory remarks are just to inform the reader that the author of this review is well aware of the particular difficulty of stimulating the interest of the space community for abundances: Space physicists, especially theoreticians, prefer to deal with a minimum of constituents, i.e., with protons and electrons. This review, however, will not paint the solar wind in black and white; it will include colors. That is, the picture includes protons and electrons and the full diversity of minor species, describing transitions of colors, mixtures, shadings, and tints as encountered when exploring compositional variations and modifications of charge states.

In geosciences, rare elements and isotopes are frequently used as tracers to follow the circulation of fluids (in hydrology) or to disentangle the historical record of geological formations. In a similar way, trace elements and isotopes can monitor many aspects of the solar wind fluid. Admittedly, the chemistry of the solar wind is simpler and exhibits not as many facets of matter as are observed, for example, in geological systems that deal with high densities at moderate temperature. Nevertheless, some "chemical" processes, for example, the exchange of electrons, play an important role in determining solar wind properties.

The purpose of this paper is to review recent achievements related to solar wind composition. The topic has gained significant interest in recent years. SOHO has provided a wealth of new data that have barely been digested by the solar community. Many questions have not been answered yet. For instance, the solar corona exhibits distinct compositional features; however, how these features transfer into the solar wind is understood only in a very crude manner. A more or less clear theoretical picture about the solar wind and the role of minor species within the wind flow existed before SOHO and Ulysses; both missions have helped to considerably narrow the parameter space for modeling the solar wind and its minor constituents above the transition region. However, this author's impression is that quite the opposite has happened with respect to the picture of processes occurring underneath. The "unified" one-dimensional picture of the chromosphere and the transition region is suffering from the complicated features revealed by the unprecedented resolution of the optical instruments on SOHO. The same applies for the compositional interpretation: Whereas elemental abundance variations in the solar wind cover typically less than an order of magnitude, much bigger abundance variations have been reported from optical observations in the source region. Is the solar wind flow fed from many tiny

[1]Also at Physikalisches Institut, University of Bern, Bern, Switzerland.

Reviews of Geophysics, 38, 2 / *May 2000*
pages 247–266
8755-1209/00/1999RG000063*$15.00*
Paper number 1999RG000063

streamlets with very different properties which are averaged out in the general solar wind flow? Or are there still serious inconsistencies in the various methods to derive abundances? For instance, is there insufficient time resolution in the particle observations or poor disentangling of line-of-sight effects in the optical measurements? Beginning with some plausible scenarios for the causes of solar wind abundance variations, this review summarizes observational facts supporting and contradicting these scenarios. It is organized in the following manner: After a short section on basic concepts a summary on abundances in the source material of the solar wind, i.e., on photospheric abundances, is given. Then, in the following sections, processes which could alter the solar matter on its way from the solar surface into interplanetary space are discussed.

2. BASIC CONCEPTS

Small-scale magnetic reconnection on the solar surface appears to be the most important source of energy to heat the solar corona. Typical maximum coronal temperatures are in the range from 1–2 $\times$ 10^6 K, at which temperatures the thermal speeds of protons and electrons are sufficient to continuously escape from the gravitational attraction of the Sun. *Parker* [1958] was the first to give a correct fluid dynamic description of the solar wind phenomenon. At the given temperatures, however, it is not self-evident that heavier particles than protons are incorporated into the outflowing proton-electron gas. Coulomb collisions [*Geiss et al*., 1970] and wave particle interaction [e.g., *Cranmer et al*., 1999] are indispensable to carrying heavy species into the interplanetary plasma.

Before entering into a more systematic discussion on solar abundances and solar system abundances, a few basic concepts need to be elaborated upon. *Anders and Grevesse* [1989] define solar abundances as "best estimates" for the Sun, or more precisely, for the solar photospheric composition. Solar system abundances, on the other hand, are best estimates for the solar system and bear great relevance as a reference for the nuclidic evolution of the galactic medium. For the following discussion it is assumed that the birth of the solar system, 4.6 Gyr ago, consisted of a unique and instant act of separation of solar system matter from the rest of the galaxy. Hence the distinction of "solar system matter" from "interstellar matter" (ISM) is meaningful for the subsequent phases of solar system evolution. Note, however, that the act of separation of solar system matter from the surroundings could have taken as much as several million years, considering the large deviations of the ^{26}Al content of some refractory meteoritic inclusions from, for example, terrestrial matter. These anomalies are difficult to explain in terms of a simple chronological sequence of events as outlined above [*Wood*, 1998].

On a lower level that involves only parts of the solar system, one has to visualize exchange of materials with the surroundings. Loss or gain of matter is frequently accompanied by fractionation or chemical differentiation. For instance, sublimation of ice or dust grains can lead to a preferential loss of volatile elements and, consequently, to a selective depletion of volatiles in the remainder. Fractionation processes could influence the elemental composition of a given reservoir as well as its isotopic composition. The loss of volatiles through evaporation is very likely to lead to an enrichment of the heavier isotopes of the partially evaporated substrate. It seems more likely, however, that the chemical segregation of planetary bodies from the solar nebula occurred through condensation, accompanied by loss of the more volatile species. The isotopic fractionation of refractory and moderately volatile elements during condensation is minimal, since the thermodynamical laws of forming compounds at elevated temperatures govern the incorporation of isotopes into the condensate, and the strongly mass dependent evaporation is not involved. *Humayun and Clayton* [1995] showed that the strong abundance variations of the moderately volatile element potassium within a wide variety of solar system samples are, within very narrow limits of experimental uncertainty, not accompanied by isotopic fractionation. Thus the partial and sometimes almost complete loss of this type of element cannot be the result of a mass-dependent evaporation process. This is important for further discussion about inferences of the isotopic composition of the Sun and of the solar wind from planetary samples.

Chemical and isotopic fractionation can also occur through the separation of an inhomogeneous mixture of gas, dust, and ice grains. Many chemical elements in the solid phases of very primitive and undifferentiated meteorites still bear the imprints of nucleosynthetic events predating the formation of the Sun. It is easy to imagine that a variable mixture of these components within the protosolar nebula will lead to isotopic heterogeneities within the solar system that will be related to the chemical composition of the samples considered. As is most clearly evidenced in the case of the D/H abundance ratio, chemical reactions, by the law of minimization of the free energy and maximization of entropy, especially at low temperatures, lead to the enrichment of heavy isotopes in the most tightly bound compounds available. Volatility is a criterion for selective chemical depletion in the condensed matter–gas transition. Another property, to be extensively discussed in the following, is the first ionization potential (FIP) of an element which plays a crucial role in the neutral-ion transition of matter occurring in the upper solar atmosphere.

3. SOLAR ABUNDANCES: THE ORIGIN OF SOLAR WIND COMPOSITION

The solar wind is fed with solar matter; hence, in a rough approximation, the average solar wind composi-

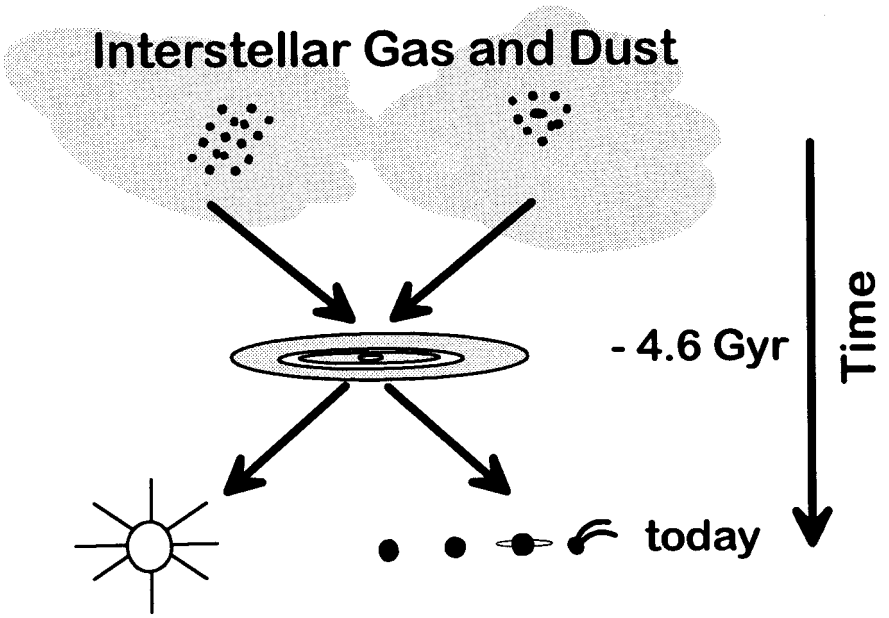

Figure 1. Crossroads of solar system formation in space and time. Solar system matter consists of a well-mixed sample of interstellar material, representative of the galaxy at ~10 kpc from the galactic center, 4.6 Gyr ago. While the Sun (or at least its convection zone) has remained largely unaltered throughout the solar system lifetime, planetary samples have undergone weaker or stronger chemical fractionation or physical fractionation, for example, involving gas/dust separation. Since the elemental and isotopic composition of interstellar gas and interstellar dust can differ substantially, physical fractionation will also lead to compositional differences among different planets, meteorite parent bodies, and comets.

tion is similar to the solar atmospheric composition or, more generally, to the solar composition, which is by number fractions 90% hydrogen, 9% helium, and approximately 0.2% heavier elements. The abundance tables of *Anders and Grevesse* [1989] are still the most popular and comprehensive reference for solar composition. This compilation and follow-ups [e.g., *Grevesse and Sauval*, 1998] are constructed on optically determined photospheric abundances. A strong improvement of the quality of solar determinations, which often have intrinsically high experimental uncertainties due to complex and uncertain model assumptions, was achieved by including abundances from refractory elements in meteorites for intercalibration. Furthermore, for some rare species, the tables use interpolations based on nucleosynthetic calculations. Merging solar photospheric and meteoritic abundances is justified by the assumption that all solar system matter originated from a well-defined and well-mixed reservoir with a standard abundance distribution (SAD) of elements and isotopes. Among meteoriticists this reference composition is sometimes called "The Holy Grail." The main difference between the photospheric and meteoritic composition consists in the depletion of volatiles in meteorites to a variable degree, depending on the petrographic classification of the sample considered. *Anders and Grevesse* [1989] showed that photospheric and meteoritic abundances that could be determined independently and with high reliability agreed for a wide range of refractory and moderately volatile elements, thus justifying their basic assumption of the commonality between solar and planetary matter.

Figure 1 illustrates the importance of solar abundances. Since the Sun is considered to contain a largely unfractionated sample of matter of the protosolar nebula as it existed 4.6 Gyr ago, it connects two reference sequences: The first is the composition of the local interstellar medium, 4.6 Gyr ago. "Local" means at a distance approximately 10 kpc (~30,000 light years) from the galactic center; and the second is the origin of the chemical and isotopic evolution of any type of planetary matter.

Evidently, both topics need a critical discussion. First, whether solar system matter can be considered as typical for the galaxy depends on the degree of galactic mixing. Generally, it is believed that because of the shortness of the galactic rotation period as compared with the galactic chemical evolutionary timescale, matter is well mixed over some range of radial distances. This assumption seems not to be contradicted by observations. Of course, local variations, for example, those related to nucleosynthetic events, such as the explosion of a supernova, could exist. If a supernova triggered the formation of the solar system, as was widely believed by geochemists in the 1970s, the solar system might deviate from typical samples of the average galactic medium. Today, opinions converge that late nucleosynthetic injections generally

played a minor role in forming solar system abundances; possibly they affected a limited number of rare isotopes.

Second, the protosolar disk might have lost some matter after the initial phases of settling toward the center plane. If present-day solar matter has been cycled through the disk, it also was influenced by such a loss in other ways. For instance, it might be chemically fractionated to some extent relative to the original composition of the protosolar nebula. According to current ideas, however, this loss did not exceed a fraction of, say, 20% of the solar mass [e.g., *Cassen*, 1996]. Depending on the efficiency of the loss mechanism and the accompanying isotopic fractionation effects and the exchange rate between disk and Sun, such a loss might be accompanied by some isotopic fractionation of the order of a per mil or so. However, for lack of more detailed information and because of the overall good match between solar and meteoritic abundances, it is generally assumed that the Sun is largely unfractionated and that solar matter is a good starting point for the study of the further evolution of meteorites and planets.

Expanding on the assumption that the Sun is largely an unfractionated sample of the protosolar nebula and of the interstellar medium 4.6 Gyr ago, investigating systematic compositional differences among solar disk objects (planetary or meteoritic) is a fascinating topic. To elaborate on mechanisms that modify disk material, studying the circumstances that affect the elemental and isotopic composition of disk objects is definitely beyond the goals of this review. For more information, consult review articles, by, for example, *Clayton* [1993] or the recent article on solar system oxygen isotope systematics by *Wiens et al*. [1999 and references therein] and the volume of the recent workshop on solar composition and its evolution [*Fröhlich et al*., 1998].

According to the standard evolutionary model of the Sun, the composition of the outer convective zone, which is reflected in its photospheric composition, has remained largely unchanged throughout the main-sequence lifetime of the Sun. There are, however, two important points to be considered: An important exception concerns the abundances of some light stable nuclei (D, ^{3}He, and the lithium nuclei) that are affected by nuclear burning at the bottom of the outer convective zone, for example, due to convective overshoot [cf. *Blöcker et al*., 1998] or rotation-induced deep mixing in an early evolutionary phase. The other important process, to be discussed separately in the following, is gravitational settling of heavy elements in the outer convective zone of the Sun [e.g., *Michaud and Vauclair*, 1991]. A third possible process, migration of chemically altered giant planets with eventual accretion on the Sun during early solar evolution, will not noticeably affect the solar surface composition because the well-mixed outer convective zone of the Sun must have been considerably deeper than today during the first few 10 Myr of disk evolution [cf. *Laughlin and Adams*, 1997]. Many of the processes and possible events outlined above would also have minor effects on the isotopic composition of the present-day outer convective zone. However, whereas isotopic variations of the order of fractions of per mils can nowadays be detected among meteoritic, lunar, and terrestrial samples, it is still not possible to determine the isotopic composition of the solar atmosphere with the necessary accuracy. The only access to such determinations is provided through the solar wind. The most important motivation from the astrophysical and geochemical viewpoint for measuring solar wind abundances is therefore creating the potential of gaining information on the isotopic composition of solar matter and, furthermore, of setting a point of reference for the isotopic evolution for the entire solar system, including planetary atmospheres, comets, meteorites, and planets. Consequently, the next goal is to ascertain the authenticity of solar wind samples to represent the present-day convection zone.

Solar wind composition and kinetic properties, for example, as observed at a distance of 1 AU, are established on very different temporal and spatial scales. Although these properties might depend on one other in a complicated manner, an attempt is made here to order them along an evolutionary sequence that begins beneath the solar surface and ranges into interplanetary space, as shown in Table 1. This spatial order also serves as a guideline for the organization of the following sections, which treat fractionation processes affecting the solar wind composition in some way. Gravitational settling occurs at the lower boundary of the convection zone. This process could influence the elemental and isotopic composition of the solar wind source material. The ion-neutral separation occurs in the upper chromosphere and mainly influences the elemental composition of the corona and the solar wind. The charge state composition is established in the inner corona as long as ion-electron collisions are sufficiently frequent to modify the ionic charge of minor species. These processes will be summarized in the final sections of this paper. Farther away from the solar surface, inefficient Coulomb drag and wave particle interaction can modify the solar wind composition, the best known case being the He/H ratio, with respect to its original source composition. Although the important processes that shape the solar wind abundances occur within $\sim 10\ R_\odot$ of the Sun, the kinetic properties of the solar wind particles continue to be modified out to the boundaries of the heliosphere. This topic, however, will not be addressed in this review.

4. FRACTIONATION PROCESSES

4.1. Gravitational Settling Through the Boundary Between the Radiative and Convective Zones of the Sun

Those evolutionary models that best reproduce the observed solar oscillations include gravitational settling in the interior of the Sun. The most important effect arises from a depletion of helium of typically 10% in the

TABLE 1. Relevant Processes and Spatial Scales for Modification of Solar Wind Composition and Kinetic Properties

Distance From Solar Surface	*Site*	*Process*	*Most Affected Solar Wind Property*
$-0.3\ R_\odot$	boundary radiative/convective zone	gravitational settling/convective mixing	elemental and isotopic composition
$<1\ R_\odot$	upper chromosphere lower transition region	ion-neutral separation	elemental composition
$1–3\ R_\odot$	inner corona	electronic collisions	ionic charge state
$1–10\ R_\odot$	upper transition region, corona	Coulomb collisions/gravitational stratification	He/H ratio, elemental and isotopic composition
$1–10{,}000\ R_\odot$	interplanetary medium	wave-particle interaction stream-stream interaction	bulk speed, ionic velocity distributions bulk speed, ionic velocity distributions

convection zone compared with its initial abundance. If this process is responsible for the depletion of helium at the solar surface over the lifetime of the Sun, it must also affect other elements, and indeed, the most sophisticated solar models [e.g., *Turcotte et al*., 1998] predict a steady depletion of all heavier elements of the same order of magnitude. The effect, however, is generally not taken into account when comparing photospheric abundances (relative to hydrogen) with other solar system abundances. This can be justified to some extent. First, there is no need to account for the effect because the uncertainties of photospheric abundances are usually larger, except for some optimistic (and therefore unrealistic) compilations. Second, the process seems to affect elements in the same mass range similarly. Hence the error introduced by using photospheric abundance ratios (except those including hydrogen) instead of using initial solar abundances is probably smaller than 10%.

The situation, however, might be quite different for the application of isotopic abundances. Although the best determinations of the isotopic composition of the solar wind still have typical uncertainties of 1–3% per mass unit [e.g., *Kallenbach et al*., 1997; *Wimmer-Schweingruber et al*., 1998], it seems likely that these uncertainties can be substantially reduced within the coming few years. The uncertainties of laboratory analyses of some isotopic ratios in planetary and meteoritic samples have reached the parts-per-million level. Hence an effect that amounts to fractions of percents, as expected from gravitational settling in the convection zone, will have to be seriously considered at some time.

The physical mechanism of gravitational settling can be visualized as the result of two opposing forces. The settling process is due to the gravitational force exerted on some minor species that is heavier than the surrounding proton-electron gas. Thus, if there was no momentum transfer (friction) between the heavy species and the surrounding gas, heavy species would rapidly drop through the solar gas into the potential well at the solar center. Owing, however, to the collisional interaction (expressed by the interdiffusion coefficients D_{12}) between the main gas and the species considered, there is only a very slow equilibrium downdrift through the boundary between the convection zone and the radiation zone of the Sun:

$$v_D = -D_{12}\left\{\frac{\partial \ln c}{\partial r} + \left[\left(A - \frac{Z}{2} - \frac{1}{2}\right)g - Ag_R\right]\frac{m_p}{kT} - k_T\frac{\partial \ln T}{\partial r}\right\} \quad (1)$$

[*Michaud and Vauclair*, 1991]. Three terms on the right-hand side of (1) describe the downdrift of particles: The first is isothermal, concentration-driven diffusion (c is the concentration of the species considered). The second term in brackets describes gravitational settling. The third term accounts for thermal diffusion. For the gravitational settling term, a species of atomic mass A ionized to an effective charge Z in the proton-electron gas is considered. The force due to gravity is partially compensated by the radiation pressure, exerted from photons emanating from the solar interior. The radiative accelerating force is given by Am_pg_R/kT. At the lower boundary of the convection zone that is of interest here, this contribution amounts to less than 10% of the gravitational force for light and medium mass elements ($A < 40$) according to *Turcotte et al*. [1998, Figures 11 and 14]. The quantity k_T in the last term is the thermal diffusion coefficient. Both normal diffusion and thermal diffusion will be neglected because the corresponding concentration gradients and thermal gradients are very small. Hence (1) simplifies to

$$v_D = -D_{12}\left[\left(A - \frac{Z}{2} - \frac{1}{2}\right)g - Ag_R\right]\frac{m_p}{kT}. \quad (2)$$

To estimate the isotope effect of gravitational settling over the lifetime of the Sun, we will rely heavily upon the results of *Turcotte et al*. [1998]. In the following, compare the downdrift speeds of two species (i, j) at the condi-

TABLE 2. Isotopic Fractionation Due to Gravitational Settling After 4.6 Gyr in the Solar Convection Zone

Element	F_{el}[a]	$\langle Z \rangle$[b]	*Isotopic Fractionation Factors*
He	0.896	2	$f_{4,3}$: 0.967[c]
C	0.914	6	$f_{12,13}$: 1.009[c]
		4	$f_{12,13}$: 1.011
N	0.916	6	$f_{14,15}$: 1.005
		5	$f_{14.15}$: 1.009
O	0.916	6	$f_{16,17}$: 1.004; $f_{16,18}$: 1.009
		5	$f_{16,17}$: 1.006; $f_{16,18}$: 1.013
Ne	0.914	10	$f_{20,21}$: 1.004[c]; $f_{20,22}$: 1.008[c]
		8	$f_{20,21}$: 1.005; $f_{20,22}$: 1.010
Mg	0.913	12	$f_{24,25}$: 1.003[c]; $f_{24,26}$: 1.007[c]
		10	$f_{24,25}$: 1.004; $f_{24,26}$: 1.008
Si	0.915	12	$f_{28,29}$: 1.003; $f_{28,30}$: 1.005
		10	$f_{28,29}$: 1.003; $f_{28,30}$: 1.006
S	0.916	14	$f_{32,34}$: 1.005; $f_{32,36}$: 1.009
		12	$f_{32,34}$: 1.005; $f_{32,36}$: 1.010
Ar	0.913	14	$f_{36,38}$: 1.004
		12	$f_{36,38}$: 1.004
Ca	0.924	14	$f_{40,44}$: 1.007; $f_{40,48}$: 1.014
		12	$f_{40,44}$: 1.006; $f_{40,48}$: 1.012
Ti	0.924	14	$f_{48,46}$: 0.997; $f_{48,50}$: 1.003
		12	$f_{48,46}$: 0.997; $f_{48,50}$: 1.003
Fe	0.914	16	$f_{56,54}$: 0.997; $f_{56,57}$: 1.001
		12	$f_{56,54}$: 0.998; $f_{56,57}$: 1.001

[a]Element depletion after 4.6 Gyr according to *Turcotte et al*. [1998, Figure 14].
[b]Estimated average charge state of element at the bottom of the convection zone.
[c]Radiative acceleration not included for fully ionized species.

tions at the bottom of the convection zone. The convection zone is certainly well mixed, and no concentration gradients will build up within it. The constant drizzle of heavy species through the boundary, however, will ultimately lead to some overall depletion of the species in the well-mixed convective layer above. Typical drift speeds are of the order of 10^{-11} m s^{-1} only. Hence it takes several lifetimes of the Sun for a particle to move across a fraction of a solar radius. For the two species i, j we obtain

$$\frac{v_{Di}}{v_{Dj}} = \frac{D_{1i}}{D_{1j}} \frac{(A_i - Z/2 - 1/2) - A_i g_R/g}{(A_j - Z/2 - 1/2) - A_i g_R/g} = \sqrt{\frac{A_j}{A_i}} \frac{(A_i - Z/2 - 1/2) - A_i g_R/g}{(A_j - Z/2 - 1/2) - A_i g_R/g}. \quad (3)$$

Note that the radiation forces do not discriminate between isotopes. This is why the same mass term appears with g_R/g in the numerator and denominator of (3). Following *Michaud and Vauclair* [1991], the following simple scheme is applied to estimate the isotopic fractionation factor:

$$f_{i,j} = \frac{c_i}{c_j}(t) \Big/ \frac{c_i}{c_j}(0). \quad (4)$$

A simple mass conservation consideration brings

$$\frac{d(c_i M_{CZ})}{dt} = -c_i v_{Di} \rho(r) \times 4\pi r^2,$$

which has the solution

$$c_i(t) = c_i(0) \exp\left(-\frac{t}{\theta_i}\right). \quad (5)$$

Here θ_i is the gravitational settling timescale:

$$\theta_i = \frac{M_{CZ}}{v_{Di} \rho(r) 4\pi r^2}, \quad (6)$$

where M_{CZ} is the mass of the convection zone and $\rho(r)$ is the mass density at its lower boundary.

Instead of computing the θ_i for different species, we adopt the elemental depletion factors $F_{\mathrm{el}} = c_{\mathrm{el}}(t)/c_{\mathrm{el}}(0)$ derived from *Turcotte et al*. [1998] and relate concentrations of isotopic species j and i by scaling the timescales with the inverse of the diffusion velocity, as suggested by (6):

$$\frac{c_i(t)}{c_j(t)} = \frac{c_i(0)}{c_j(0)} \exp\left[-\frac{t}{\theta_i}\left(1 - \frac{v_{D,j}}{v_{D,i}}\right)\right], \quad (7)$$

whereas from (5),

$$F_i = \exp\left(-\frac{t}{\theta_i}\right) \quad (8)$$

is taken for the elemental depletion (or more precisely, for the depletion of the most abundant isotope of an element) and used to replace the factors $\exp(-t/\theta_i)$ in (7). Finally, the isotopic fractionation factor is expressed with the simple relation

$$f_{i,j} = F_{\mathrm{el}}^{(1-(v_{D,j}/v_{D,i}))}. \quad (9)$$

Table 2 gives isotope fractionation factors after a solar main-sequence lifetime of 4.6 Gyr for the convection zone of the Sun; $f_{i,j} > 1$ means that the species with the atomic mass i will be enriched by the factor $f_{i,j}$ over species j compared with their initial abundances. First, it is worth noting that gravitational settling is not simply mass dependent. Second, although modifying the average charge $\langle Z \rangle$ does not have a strong impact on the isotopic fractionation factors, it is instructive to note in Table 2 the "levitating" effect of strong ionization at the lower boundary of the convection zone.

This levitating effect is the reason for fractionation factors being larger than estimated from consideration of mass ratios only. Similarly, radiation forces tend to increase the fractionation factors even more strongly. According to (3), in an extreme (and unrealistic) case one isotopic species of a given element could experience a net lifting force, whereas the other would still drift downward. Although according to Table 2 practically all factors differ by less than a percent from 1, an experimental verification, for example, of the effect on the ^{24}Mg/^{26}Mg ratio under favorable solar wind conditions, seems attainable with isochronous mass spectrometers

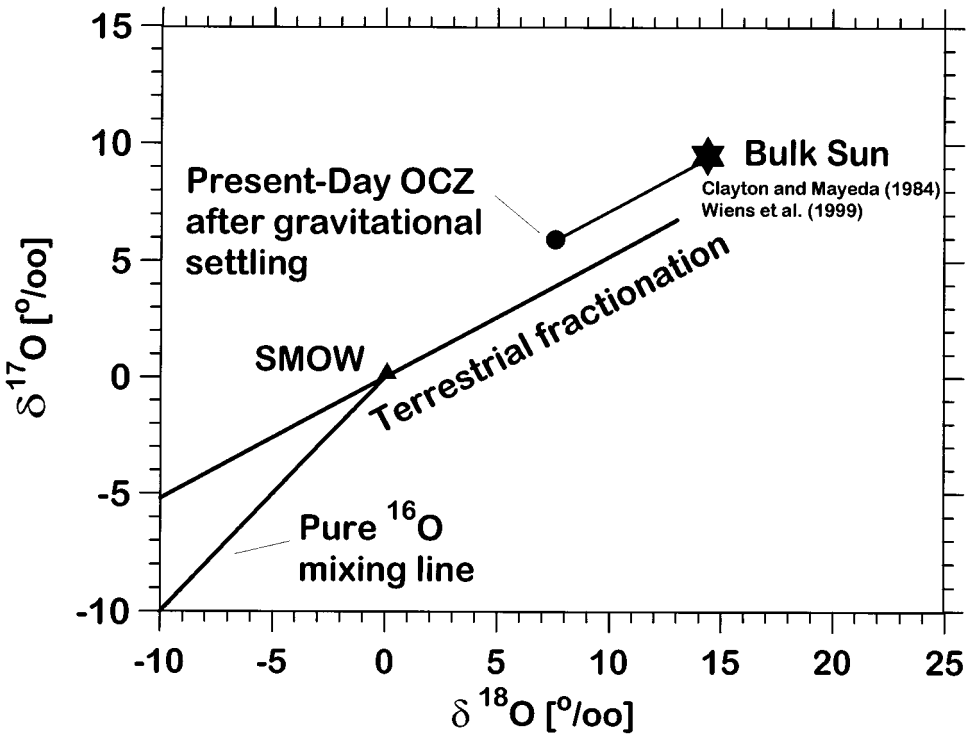

Figure 2. Oxygen isotope systematics (adapted from *Wiens et al*. [1999]). The bulk Sun estimate (six-sided star) is derived from measurements of the Murchison carbonaceous chondrite. The solid triangle "SMOW" indicates the reference value which is "standard mean ocean water." Gravitational settling of oxygen would deplete the heavy isotopes by 4.5‰ and 8.8‰, respectively (see Table 2), leading to a composition of the convection zone as indicated by the solid circle after 4.6 Gyr. The delta notation is used to indicate variations with respect to SMOW (e.g., $\delta^{18}O_{sample}[‰] = ([^{18}O/^{16}O]_{sample} - [^{18}O/^{16}O]_{SMOW})/[^{18}O/^{16}O]_{SMOW} \times 1000$).

such as the Charge, Element and Isotope Analysis System/mass time of flight sensor (CELIAS/MTOF) on SOHO [*Hovestadt et al*., 1995].

The Genesis mission of NASA will use the foil collection technique to determine the isotopic composition of several elements including oxygen in the solar wind. *Wiens et al*. [1999] have recently made an attempt to extrapolate the isotopic composition of solar oxygen from meteoritic data. Assuming their bulk Sun estimates and taking into account the isotopic fractionation effect due to gravitational settling as given in Table 2, one obtains an estimate for the convection zone after 4.6 Gyr (and the photosphere), as given in Figure 2. The effect of gravitational settling is of the order of a percent and seems tiny in comparison with the present-day experimental uncertainties of solar wind measurements. It is significant, however, in the context of solar system oxygen isotope systematics.

At this point a note of caution in the general discussion of gravitational settling in the convection zone is appropriate: Although solar models that involve a secular depletion of helium and heavier elements reproduce the helioseismological observations better than models not involving this effect, the effect could in reality be strongly reduced or vanish altogether if convective overshooting is more important than anticipated in the standard solar model. A scenario to deplete Li during the entire solar main-sequence lifetime [*Blöcker et al*., 1998] would factually increase the mass of the convection zone and hence substantially dilute the effect of gravitational settling. Moreover, one might question whether the idealized gravitational settling scenario, as outlined above, is realistic in a partially magnetized and partially turbulent environment such as the convection zone.

4.2. Elemental Fractionation in the Ion-Neutral Separation Process (Observations)

4.2.1. Coronal abundances derived from solar energetic particles. The supply of ionized matter from the generally neutral solar atmosphere to the corona plays a crucial role in establishing solar wind abundances. Since ionization of elements with different atomic properties is involved, it is natural that these atomic properties are relevant for the replenishment of ions into the corona. From the systematics of coronal abundances, for example, as derived from solar energetic particles (SEPs) or from solar wind ions, compared with the photospheric abundances, it appears that the first ionization potential (FIP) is the most important atomic parameter. Figure 3 illustrates the FIP dependence of coronal abundances as derived from solar en-

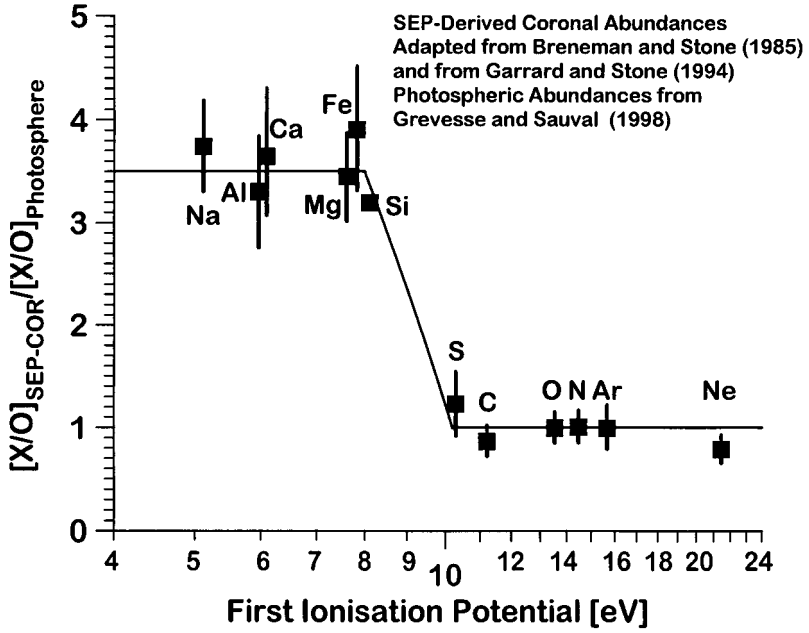

Figure 3. Solar energetic particle derived coronal abundances relative to photospheric abundances and normalized to the oxygen abundance (the so-called first ionization potential (FIP) plot). The solar energetic particle (SEP) derived abundances are from *Breneman and Stone* [1985] using an improved Q/M fractionation law [*Garrard and Stone*, 1994]. The photospheric abundances are from *Grevesse and Sauval* [1998].

ergetic particles [*Breneman and Stone*, 1985; *Garrard and Stone*, 1994]. The abundances have been put in relation to photospheric abundances as given by *Grevesse and Sauval* [1998]; both sets are normalized with the abundance of oxygen. A step pattern, indicated by horizontal lines to guide the eye, emerges: Elements with low FIP, i.e., FIP below the Lyman α limit at 10.2 eV, are generally overabundant by a factor of 3–5 in the equatorial corona; and elements with FIP > 10.2 eV show no enrichment in comparison with the photosphere.

4.2.2. Solar wind abundances. Figure 4 shows solar wind abundance data from typical low-speed, inter-

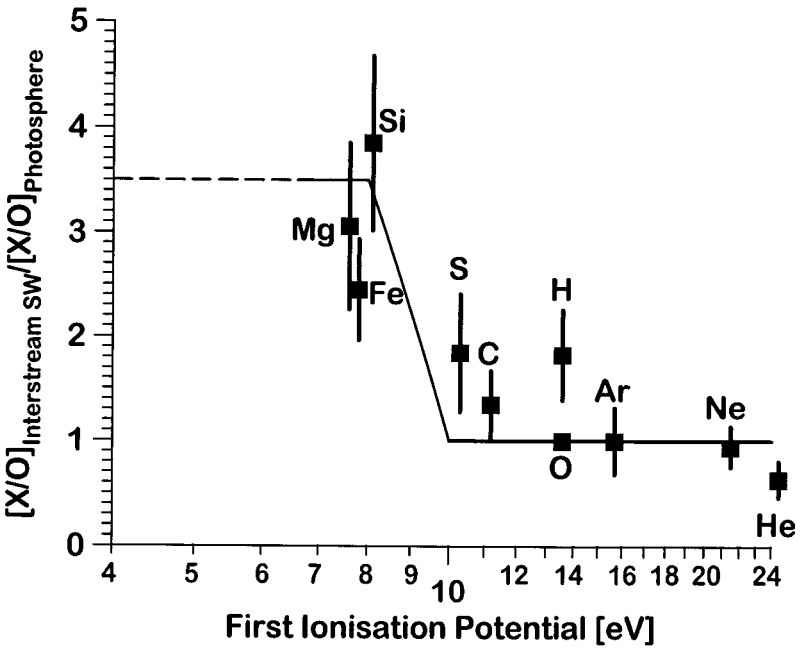

Figure 4. Interstream solar wind abundances normalized with oxygen relative to photospheric abundances as given by *Grevesse and Sauval* [1998].

stream solar wind that emanates from the equatorial streamer belt. The format of Figure 4 is the same as for Figure 3. Although a pattern similar to that found for the SEP-derived coronal abundances can be recognized in this type of solar wind, it appears that the step is less pronounced, and certainly, the low FIP plateau is not so well defined as in the case for the SEP-derived corona. This impression is partly due to the generally larger experimental uncertainties of the solar wind data. Some caution is appropriate in any case: The SEP-derived coronal values have been corrected for a systematic charge per mass (Q/M) fractionation that is normally observed in shock accelerated particles. The correction factor amounts to typically some tens of percents for individual element abundances and rests on the photospheric determination of a few low-FIP elements such as Ca and Fe. Furthermore, it has become clear [e.g., *Reames*, 1998] that gradual flare events also produce some enrichment in heavy species which does not necessarily follow the Q/M systematics traditionally ascribed to the impulsive flares.

Coronal hole–associated solar wind appears to be less FIP fractionated than interstream solar wind. The enrichment of low-FIP elements relative to the high-FIP elements amounts to typically a factor of 2 [e.g., *Geiss et al*., 1995], depending on the adopted photospheric abundances [*Aellig et al*., 1999; *Ipavich et al*., 1999].

The FIP bias of Fe in Figure 4 seems less pronounced than for the other low-FIP elements. This can possibly be attributed to the photospheric Fe/O abundance ratio, which has been taken from the table of *Grevesse and Sauval* [1998]. H. Holweger and coworkers [see *Aellig et al*., 1999] have made an attempt to derive a photospheric Fe/O ratio directly from observations of various lines, thereby eliminating model uncertainties and some uncertainties due to atomic physics. The revised value is approximately 25% lower than the value given by *Grevesse and Sauval* [1998], and consequently, the Fe value in Figure 4 lies closer to the plateau together with Si and Mg. In order to remain consistent, however, Figure 3 should also be redrawn, taking into account a different Q/M bias and lifting the coronal Fe abundance significantly above the high-FIP plateau.

4.2.3. Interpretation of the FIP effect. Major chemical elements prevail predominantly as neutrals in the photosphere. They begin to ionize in the overlying chromosphere due to exposure to the coronal ultraviolet radiation, and it is here, at the site of neutral-ion conversion, where the FIP effect must occur.

However, a comprehensive and self-consistent physical picture of the sites of ion-neutral separation does not exist [cf. *Judge and Peter*, 1998]. Possibly, because at this site the transition occurs from predominantly neutral material (in the photosphere) to fully ionized plasma (in the corona) containing a large amount of latent recombination energy, one finds a complex, structured, turbulent, partially magnetized medium eluding a self-consistent physical description. Magnetic flux tubes are rooted in the photosphere. Owing to the requirement of pressure balance, material contained in magnetically dominated structures is generally tenuous, it floats on the photosphere, and it is driven with the magnetic structures attached to the sites of downwelling ionized matter. Here flux tubes concentrate. In the upper chromosphere, which is also in hydrostatic equilibrium, the gas pressure is orders of magnitude lower while the magnetohydrodynamic pressure has decreased only weakly. Flux tubes therefore expand to form the so-called canopy, and a more homogeneous medium emerges. Evidently, the turbulent motion of flux tubes at the bottom of the chromosphere leads to field line merging, which will eventually heat the layer. However, this description seems to be rather idyllic compared with the scenario of *Carlsson and Stein* [1995], who portray a chromosphere reminiscent of a stormy sea. In their chromosphere, temperatures vary typically over an order of magnitude within 100 s, rendering any steady state treatment of the ion-neutral separation process unbelievable.

Nevertheless, virtually all models describing FIP fractionation quantitatively have to resort to some stationary or "average" picture of the physics involved. In view of the dynamic nature of the ion-neutral separation environment, it is not surprising that the first ionization time is a better ordering parameter to describe the FIP fractionation than the first ionization potential [*Geiss*, 1998]. Once this has been established, the next step to obtaining an enrichment of quickly ionizing species is to separate these species from neutrals and feed them into the corona. Many models use magnetic or electric fields to separate ions from neutrals at their site of production and to feed them into the corona [*Geiss and Bochsler*, 1985; *von Steiger and Geiss*, 1989]. In other models, magnetic fields are of minor importance, and Coulomb drag exerted by protons on minor species is used to drive ions effectively out of the ionization site [*Marsch et al*., 1995; *Peter*, 1996]. If the ionization time is the ordering parameter, however, why then does the solar wind consist not only of species such as Ca, Al, and Na, which have extremely short ionization times and which are already ionized to a significant fraction, even at the low temperatures in the photosphere? Obviously, another process limits the supply of fast ionizing or preionized species into the corona. Depending on the efficiency of the transport to the site of fractionation, a species will be enriched or depleted. Since the collisional cross section of a given charged species with some neutral main gas is generally larger than the cross section of the corresponding neutral species with the same main gas particle, and since the microscopic mobility of a charged species is generally reduced in a magnetized medium, this is probably the part where the explanation for the flux limitation of ultralow-FIP elements has to be found. Transport of ions and neutral species through partly ionized matter can simply be treated as a diffusion problem. It seems, however, more likely that in addition to microscopic diffusion, turbulent motion is somehow involved. Table

TABLE 3. Synopsis of Steps in the First Ionization Potential Fractionation Process

Step	*Process*	*Reference*
Ionization	Collisional excitation and photoionization at moderate temperatures	3
	EUV photoionization and collisional ionization	1, 2, 5, 8
Transport to site of separation	Diffusion of neutrals	2, 5
Ion-neutral separation	Pressure gradients across magnetic flux tubes	1, 2
	Gravitational settling in the chromosphere	4
	Coulomb drag of minor species with protons in the chromosphere	5, 6, 8
	MHD waves	7, 8

References are 1, *Geiss and Bochsler* [1985]; 2, *von Steiger and Geiss* [1989]; 3, *Henoux* [1998]; 4, *Vauclair and Meyer* [1985]; 5, *Marsch et al*. [1995]; 6, *Peter* [1996]; 7, *Tagger et al*. [1995]; and 8, *Schwadron et al*. [1999].

3 gives an overview of the features of some existing models. The degree of elaboration differs very much among the various models. Whereas a few [*von Steiger and Geiss*, 1989; *Marsch et al*., 1995; *Peter*, 1996; *Schwadron et al*., 1999] make quantitative predictions, many others discuss processes leading to the FIP effect in a more qualitative manner.

An interesting contribution has recently been proposed by the Michigan group [*Schwadron et al*., 1999; *Zurbuchen et al*., 1998]. In this model the slow solar wind is supplied from large loop structures which are rooted in a partially ionized medium. Ions are efficiently heated and replenished due to the wave-particle interaction at the foot points, and consequently, their scale height in the loop becomes large compared with the scale heights of neutrals. In some aspects the model is reminiscent of the earlier models of *Marsch et al*. [1995] and *Peter* [1996]; some aspects seem more appealing because of the more realistic description of the physical setup. However, this is just the aspect that might lead to criticism. These authors admit that there are several free parameters, and they give no explanation why the FIP bias in the slow solar wind should be constrained to a range of values between 3 and 5. The model reproduces a realistic variability of the low-FIP abundances, but this is achieved by a somewhat questionably small variation in a range of $\pm 10\%$ of three essential free parameters, i.e., the base level of the loops within the photosphere, the wave-particle interaction rate, and the particle density within the loops. It is a general feature of FIP models: The more specific they are in defining the physical conditions, the more vulnerable to criticism for lack of realism they become.

The Michigan model merits further investigation because it possibly contains an explanation for the recently discovered strong ^{3}He enrichments that have been observed in some very rare events associated with coronal mass ejections [*Gloeckler et al*., 1999; *Ho et al*., 2000]. With resonant wave heating at foot points of loops that have been enriched in helium due to gravitational settling, a process similar to the mechanism proposed by *Fisk* [1978] for the strong ^{3}He enrichments in impulsive flares might be involved. There is no reason why moderate enrichments of ^{3}He due to resonant heating could not occur at lower energies as well. It is clear that an enrichment of the ^{3}He/^{4}He ratio over several orders of magnitude is unlikely to happen at the large particle fluxes encountered in the keV–nucleon range. However, the process begins at thermal energies and has to work through all energies up to the energies of MeV–nucleon encountered in impulsive flares [see, e.g., *Riyopoulos*, 1991; *Temerin and Roth*, 1992]. If this conjecture about the responsible acceleration process is substantiated, some mild enrichments of heavy species and concomitant isotope effects have to be expected as well in coronal mass ejection related solar wind and possibly in the slow solar wind in general [*Bochsler and Kallenbach*, 1994].

4.2.4. Isotope fractionation in the FIP process. In the models of *von Steiger and Geiss* [1989], *Marsch et al*., [1995], and *Peter* [1996] the FIP process is almost exclusively related to atomic properties, i.e., the ionization time and the collisional cross sections of neutrals in a partially ionized medium; hence mass plays only a minor role in these models. *Marsch et al*. [1995] give a particularly simple expression for the enrichment of low-FIP ions in the slow solar wind:

$$f_{jk} \approx \left(\sqrt{\frac{\tau_k}{\tau_j}} \right) \left(\frac{r_{k,H}}{r_{j,H}} \right) \left(\frac{A_j + 1}{A_j} \frac{A_k}{A_k + 1} \right)^{1/4}. \qquad (10)$$

Again, the fractionation factor f_{jk} gives the overabundance of species j relative to species k in the corona, if compared with photospheric abundances of j and k. The first factor on the right-hand side of (10) indicates that species with short ionization times are preferentially incorporated into the solar wind. The second and third sets of parentheses on the right-hand side of (10) describe the relative diffusion ranges of the species i and j with masses A_i and A_j in a neutral hydrogen gas. Species with small collisional radii have a higher probability of being fed into the solar wind. The mass of the particles enters only with a power of 1/4. Even for the extreme mass ratio of ^{3}He/^{4}He, a value $f_{3,4} = 1.016$ is expected according to (10). Similarly, the models of *von Steiger and Geiss* [1989] predict a very weak enrichment of ^{3}He

over ^{4}He in the solar wind relative to photospheric abundances.

As indicated above, some more substantial isotopic fractionation effects could occasionally be encountered, especially in slow solar wind, if selective resonant ion cyclotron heating, for example, in the context of the Michigan model [*Schwadron et al*., 1999], becomes important. Recently, several studies, essentially all related to solar energetic particles or suprathermal solar particles, have been published [*Mason et al*., 1994; *Bochsler and Kallenbach*, 1994]. None of these publications makes quantitative predictions about the enrichment factors and their correlation with the occasional ^{3}He enrichment because there are many free parameters involved. Such predictions depend crucially on the charge state of the heavier species. One species which matches exactly the second harmonic of the $^3He^{++}$ cyclotron frequency is $^{15}N^{5+}$. The study of *Bochsler and Kallenbach* [1994] predicts a strong enhancement of the $^{15}N/^{14}N$ ratio in impulsive flares and some enhancement of $^{22}Ne^{8+}$.

Whereas the latter has meanwhile experimentally been confirmed [*Williams et al*., 1998], no conclusive evidence has yet been obtained for the isotopic fractionation of nitrogen. In any case, as discussed at the end of section 4.2.3, such effects should be much smaller in coronal mass ejection–related solar wind and in slow solar wind, since, generally, impulsive flare-type resonant wave-particle heating seems to play a much less important role in these solar wind regimes. In fact, ^{26}Mg, which is also a candidate for a ^{3}He-correlated enrichment [*Williams et al*., 1998], has been found to remain within an uncertainty of 5% consistent with solar system isotopic abundances [*Wimmer-Schweingruber et al*., 1999].

4.3. Coronal Abundances Versus Solar Wind Abundances

In a simplistic view, the corona consists of matter which is in transit from the photosphere to interplanetary space, i.e., solar wind matter. In this picture, in which coronal matter cannot return to the Sun, the flux of any species through the inner corona must equal its global solar wind flux at infinity. Consequently, if all species flow with equal speed through the corona, the coronal composition agrees with the average solar wind composition. Now optical observations from SOHO have confirmed that obviously not all species flow with equal speed through the inner corona [*Kohl et al*., 1998]. Consequently, this leads to compositional variations within the corona, and when the term "coronal abundances" is used, one has to be careful in choosing the necessary weighting procedure. A general difficulty in dealing with fractionation in theoretical models is the definition of the fractionation factor that has to be introduced when comparing flux ratios with abundances in a static reservoir. *Bodmer and Bochsler* [1998] treat the problem considering a flux tube which taps a static reservoir at an arbitrary location. They define the fractionation factor over the distance between r_0 and r with $f_{jk}(r, r_0)$, relating fluxes at a remote location r with the densities of species j and k at the input location r_0.

$$f_{jk}(r, r_0) = \frac{\phi_j(r)}{\phi_k(r)} \frac{n_k(r_0)}{n_j(r_0)}. \tag{11}$$

It is a fact that the flux speeds among minor species in the solar wind in the interplanetary medium at 1 AU differ by much less than the fractionation factors of interest [e.g., *Schmid et al*., 1987; *Bochsler*, 1989; *Hefti et al*., 1998]. Fluxes are therefore often directly related to densities at 1 AU:

$$f_{jk}(r, r_0) = \frac{\phi_j(r)}{\phi_k(r)} \frac{n_k(r_0)}{n_j(r_0)} = \frac{n_j(r)}{n_k(r)} \frac{v_j(r)}{v_k(r)} \frac{n_k(r_0)}{n_j(r_0)} \approx \frac{n_j(r)}{n_k(r)} \frac{n_k(r_0)}{n_j(r_0)}. \tag{12}$$

In this presentation, fractionation appears as the result of a diffusion process that consists in essence of a comparison of probabilities of different species being transmitted through a barrier. The approach was discussed in more detail in the context of the FIP effect. The physics involved in the acceleration process is quite different. In the critical acceleration region, however, the assumption that a particle, once it is in a flux tube, is never lost again is not fulfilled. It then critically depends on the velocities of the respective species whether they will be enriched or depleted at the end of the flux tube. Hence the specific efficiency of the acceleration mechanism in the corona is crucial for the final abundance of a species in the solar wind. Even if a continuity condition is fulfilled above a critical point, high velocity of a species below this point does not necessarily mean low abundance of the species at infinity. *Bodmer and Bochsler* [1998] investigated the role of the Coulomb drag, whose variable efficiency has been made responsible for the sometimes fluctuating and sometimes strongly reduced helium-to-hydrogen abundance ratio in the solar wind. Coulomb drag might be important in accelerating heavy species in the low-speed solar wind emanating from the equatorial streamer belt. If the occasional helium depletion in the equatorial current sheet to He/H abundance ratios as low as 0.01 [*Borrini et al*., 1981] is indeed caused by the special magnetic field topology and the concomitant inefficiency of Coulomb drag in the inner corona, as proposed by *Bürgi* [1992], then isotopic fractionation effects of the order of 30% have to be expected for the ^{3}He/^{4}He ratio. *Bodmer and Bochsler* [1998] give an expression which is useful for estimating the magnitude of the isotope fractionation effects associated with inefficient Coulomb drag. Relating the isotopic abundances to the speed of the relevant species in the acceleration region as indicated by (12), the relative enrichment can be expressed as

$$f_{ij} = \left(1 - \frac{C_p^* H_i}{\Phi_p}\right) \Big/ \left(1 - \frac{C_p^* H_j}{\Phi_p}\right). \tag{13}$$

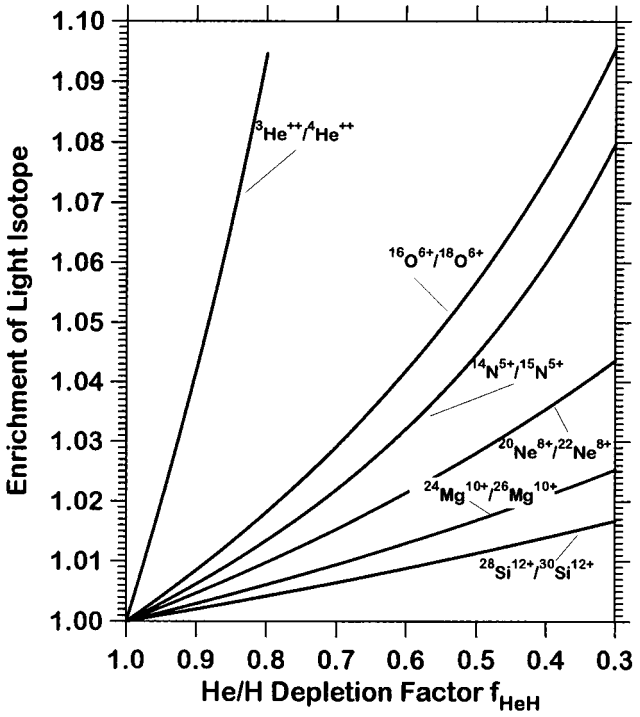

Figure 5. Expected isotope fractionation factors associated with He/H depletion factors. For instance, a depletion of He/H to 30% of its normal value in the equatorial streamer belt implies an enhancement of the $^{28}Si^{12+}/^{30}Si^{12+}$ ratio up to 1.7% over its normal coronal value.

Here Φ_p is the proton flux integrated over the full space in units of [s^{-1}], i.e., $\Phi_p = n_p v_p r^2$; H_i is the Coulomb drag factor of an atomic species with mass A_i and effective charge Z, i.e.,

$$H_i = (2A - Z - 1)/Z^2\sqrt{(A+1)/A};$$

and C_p^* is a numerical factor in units of seconds, which basically relates the electrostatic interaction of the minor species with protons to the solar gravitational attraction experienced by the particle:

$$C_p^* = \frac{GM}{2}\left(\frac{4\pi\varepsilon_0}{e^2}\right)^2 \frac{(2kT_p)^{3/2}}{\ln\Lambda}\frac{3}{16}\frac{\sqrt{m_p}}{\sqrt{\pi}}.$$

Order-of-magnitude estimates of the isotopic fractionation due to inefficient Coulomb drag can then be obtained as follows: With the assumption that an occasional depletion of He relative to H in the streamer belt is caused by lack of Coulomb drag and inserting a given He/H depletion factor $f_{\mathrm{He,H}}$ into expression (13), one uses the unknown factors C_p/Φ_p to adjust the desired He/H depletion. For any given isotope ratio of species i and j one then finds

$$f_{ij} = \frac{1 - H_i(1 - f_{\mathrm{HeH}})/1.4}{1 - H_j(1 - f_{\mathrm{HeH}})/1.4}. \qquad (14)$$

H_i and H_j are the Coulomb drag factors of species i and j as given before. An illustration of the isotope effects related to Coulomb drag efficiency and the accompanying helium depletion is shown in Figure 5.

Another process with a potential to produce weak fractionation effects is selective heating and acceleration of minor species by resonant ion cyclotron heating below the critical point. In a steady state picture of the solar wind flow, species that are preferentially accelerated will travel at faster velocities and could be somewhat enriched relative to other species. To explore the order of magnitude of this effect, a simple, one-fluid, isothermal Parker model of the solar wind is used.

The momentum equation containing a wave acceleration term $a_w\rho$ is given by

$$\rho u\frac{du}{dr} = -\frac{dp}{dr} - \frac{GM_{\mathrm{sun}}\rho}{r^2} + a_w\rho. \qquad (15)$$

Mass conservation is treated with

$$\nabla(\rho u) = \frac{1}{r^2}\frac{\partial}{\partial r}(r^2\rho u) = 0, \qquad (16)$$

and instead of the more general polytrope approximation, the most simple isothermal description is applied:

$$P/\rho = \mathrm{const} = \frac{kT}{m}. \qquad (17)$$

This set of equations is reduced to the momentum equation after eliminating ρ, and P with (16) and (17)

$$\frac{d\ln u}{dr} = \left(\frac{2kT}{m_r} - \frac{GM_{\mathrm{sun}}}{r^2} + a_w\right)\Big/\left(u^2 - \frac{kT}{m}\right), \qquad (18)$$

which can be integrated analytically. The simplest, but for this application still satisfactory, solution is found when a_w is of the form a/r^2. At the critical point $r = r_c$ the velocity reaches its critical value $u = u_c = \sqrt{kT/m}$. At this point, $r = r_c = (GM + a)/2u_c^2$, and both, denominator and numerator, vanish. Using $u = u_c$ at $r = r_c$ as initial condition for the integration of (18) yields the following solution:

$$\left(\frac{u}{u_c}\right)^2 = 1 + \ln\left(\frac{u}{u_c}\right)^2 + 4\ln\left(\frac{r}{r_c}\right) + 4\left(\frac{r}{r_c} - 1\right). \qquad (19)$$

The dissipative acceleration of species according to *Isenberg and Hollweg* [1983] is

$$a_i \sim \left(\frac{A_i}{Z_i}\right)^{\gamma-2}\left(\frac{\omega}{k_\parallel} - v_{oi\parallel}\right). \qquad (20)$$

This expression is used to scale the wave acceleration term a_w in the differential equation (18) to obtain an order-of-magnitude estimate of differences in speed among different species at the critical radius. This difference in speed below the critical point serves as an approximation for the final depletion or enrichment in the solar wind, as shown in Figure 6. It is the result of a crude and qualitative approach, since heating will affect the flow properties of different species in different ways. Because different species will have different critical

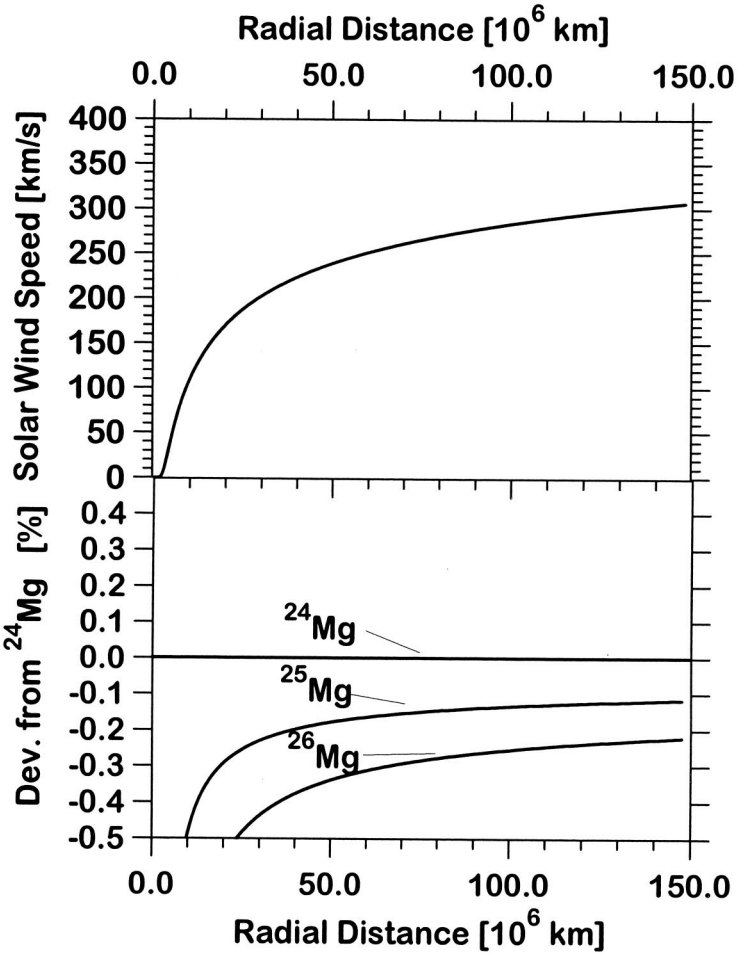

Figure 6. Scaling of speeds and estimate of typical fractionation effects among isotopic species of magnesium under the influence of wave-particle interaction in the inner corona.

points, they also will have different temperatures. All these effects cannot be treated adequately by an isothermal model. SOHO/UVCS (Ultraviolet Coronagraph Spectrometer) and SOHO/SUMER (Solar Ultraviolet Measurement of Radiation) have provided much better diagnostics than were previously available about the kinematic properties and the flow behavior of minor species [e.g., *Kohl et al*., 1998; *Tu et al*., 1998]. Undoubtedly, sophisticated theoretical models will be developed in the near future to account for the observations and to predict more subtle differences among the properties of isotopic species in an adequate manner.

5. CHARGE STATE EQUILIBRATION

The charge state distribution of minor ions in the solar wind is frequently used as an indicator for the electron temperature of the inner corona. Minor ions moving through the corona experience interactions with free electrons, leading to ionization or recombination. Photoionization is not important under normal circumstances. The details were first worked out by *Hundhausen et al*. [1968]. A comprehensive discussion has also been presented by *Owocki et al*. [1983]. The evolution of the charge state distribution of ions traveling through the corona with radially decreasing electron density and radially varying electron temperatures is described by a simple set of balance equations. Consider reactions of the following type in a steady outflowing solar wind:

$$X^i + e \rightarrow X^{i+1} + e + e \tag{21}$$

$$X^i \leftarrow X^{i+1} + e. \tag{22}$$

The balance of particles requires for a given ionization state i of the chemical species X

$$\nabla(n_i u_i) = n_e[n_{i-1}C_{i-1} + n_{i+1}R_{i+1} - n_i(C_i + R_i)], \tag{23}$$

where n_i is the particle density of species i at a given location, n_e is the (radially dependent) electron density, and C_i and R_i are the collisional ionization and recombination rates [m^3 s^{-1}] of species X^{i+}. Naturally, the ionization rate is linked to the ionization potential of the species and depends strongly on the electron temperature, whereas the recombination rate is only weakly temperature dependent. This fact is used for remote temperature diagnostics in the following way: Two species i and $i + 1$ couple via ionization (C_i) and recombination (R_{i+1}) with one other. The characteristic time

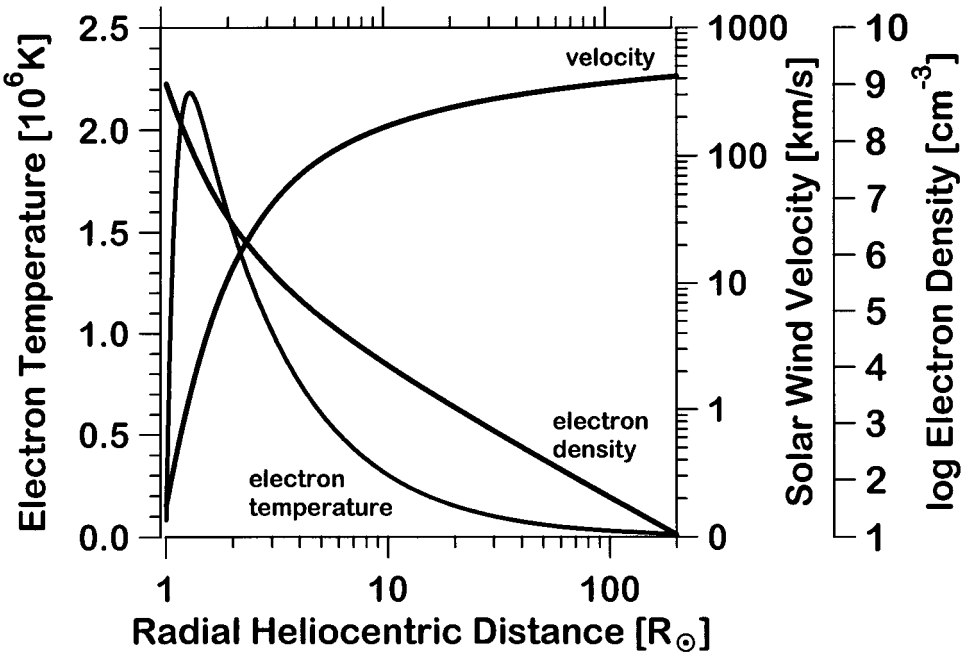

Figure 7. Radial profiles of coronal electron temperature, ion velocity, and electron density underlying charge state evolution illustrated in Figures 8 and 9.

with which these species interact with each other is determined via the ionization-recombination time

$$\tau_{i\leftrightarrow i+1} = \frac{1}{n_e(C_i + R_{i+1})}. \tag{24}$$

Owing to the rapid decrease of the electron density, this characteristic time strongly increases with increasing distance from the Sun. The characteristic coronal expansion time is defined by the time it takes the species i and $i + 1$ to travel through an electron density scale height:

$$\tau_{\exp} = \frac{H}{u}. \tag{25}$$

Aellig et al. [1997b] have given a simple scheme to parameterize the solar wind flow in the inner corona using power laws for all relevant functions.

To illustrate the charging of minor ions in the transition region and the final freezing of the charge states in the corona, a simple, home-made description of the corona involving analytical solutions like those given for the ion velocities (equation (19)) is used in the following. Note that this treatment is only to be used as a parameterization to produce realistic electron temperature profiles. Since it deals with a static electron distribution, it is certainly not consistent with Parker-type approximations, which have been used to estimate the contribution of wave acceleration to isotopic fractionation in the previous section.

For the radial electron temperature profile, one obtains a parameterization, assuming a steady state solution of the heat conduction equation with a radially dependent heating term

$$D\Delta T = -Ae^{(r_0-r)/\lambda}, \tag{26}$$

which has the general solution

$$T(r) = -\frac{A}{D}e^{r_0/\lambda}\left[\left(\frac{2\lambda^3}{r} + \lambda^2\right)e^{-r/\lambda}\right] + B + C/r. \tag{27}$$

Here D is a (constant) diffusion coefficient, describing the heat transport within a spherically symmetric corona. This crude approximation is probably as far from reality as many more sophisticated heat transport equations which assume, for example, Spitzer conductivity, in view of the great problems with the treatment of energy transport in the highly turbulent, wave-driven magnetized coronal plasma. The heating term implies an energy input which decays exponentially with radial distance. For the boundary values, $T(\infty) = 0$ and $T = T_0(R)$ (at the solar surface) are assumed, which leads to a temperature profile:

$$T(r) = T_0\frac{R}{r} + \frac{A\lambda^2}{Dr}e^{r_0/\lambda}[(2\lambda + R)e^{-R/\lambda} - (2\lambda + r)e^{-r/\lambda}]. \tag{28}$$

In this procedure, essentially three free parameters describe the profile, the temperature at the coronal base T_0, the maximum temperature contained in the term $(A\lambda^2/D)e^{r_0/\lambda}$, and the width of the temperature maximum, which is characterized by the parameter λ. The electron density is then obtained from flux conservation and a velocity profile as illustrated with (19). The profiles of velocity, electron temperature, and electron density are shown in Figure 7.

The system of charge balance equations (23) is nu-

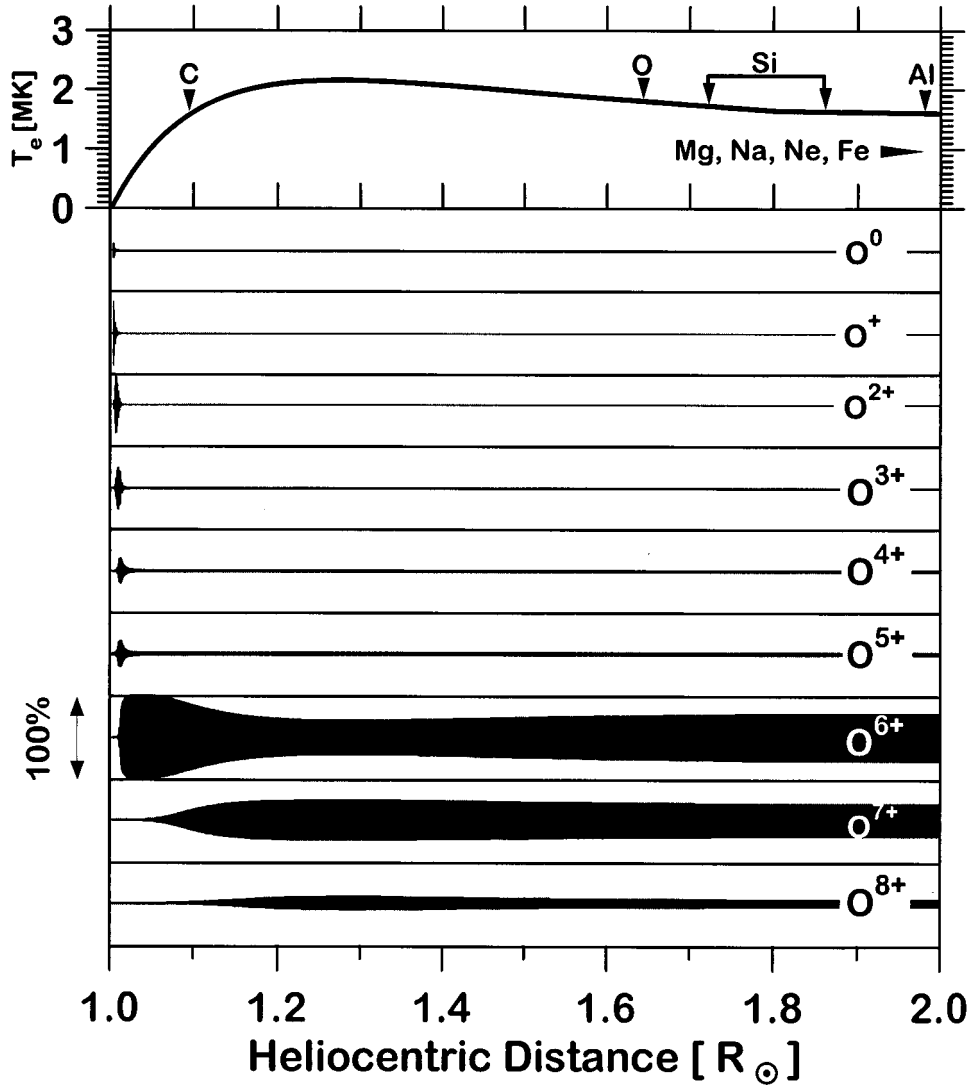

Figure 8. The top panel shows the underlying parameterization of coronal electron temperatures and the approximate location of freezing of various elements. The lower panels show the charge evolution of oxygen with distance from the center of the Sun. Neutral oxygen is injected at the solar surface. The charge state is rapidly modified over all intermediate states into O^{6+}. Beyond the temperature maximum near 1.3 $R_\odot$, the charges "freeze" and remain essentially O^{6+}, O^{7+}, and O^{8+}.

merically integrated using a procedure suitable for systems of stiff differential equations and using the ionization rates of *Arnaud and Rothenflug* [1985] and *Arnaud and Raymond* [1992]. The evolution of the charge states of oxygen ions along a radial range from 1 to 2 $R_\odot$ heliocentric distance is shown in Figure 8. The "dinosaur plot" bears its name because of its resemblance to schemes used in paleontology. Oxygen is injected in neutral form near the solar surface at a temperature of 20,000 K. The charge state quickly converts to 2+. After short phases of O^{3+}, O^{4+}, and O^{5+} dominance, oxygen prevails as O^{6+} just below the site of maximum temperature. Near the maximum a sizable fraction is converted into almost fully ionized O^{7+} and into O^{8+}. After 1.3 $R_\odot$, just beyond the temperature maximum, the charge states no longer "communicate" with each other, and despite the continuously decreasing electron temperature, the ionization state of oxygen remains "frozen" because collision-induced ionization and recombination processes stop at the low and steadily decreasing electron densities in the outer corona. Since the charge states of minor ions remain frozen throughout the heliosphere, charge state observations with particle instruments at any point in the heliosphere can provide important information about the electron temperature profile of the inner corona. Often abundance ratios determined in situ such as $n(O^{7+})/n(O^{6+})$ are expressed in the form of "electron freeze-in temperatures," for example, $T_f(O^{7+}/O^{6+})$, whereby the static equilibrium electron temperature represents the temperature where ionization of O^{6+} and recombination of O^{7+} proceed at equal rates.

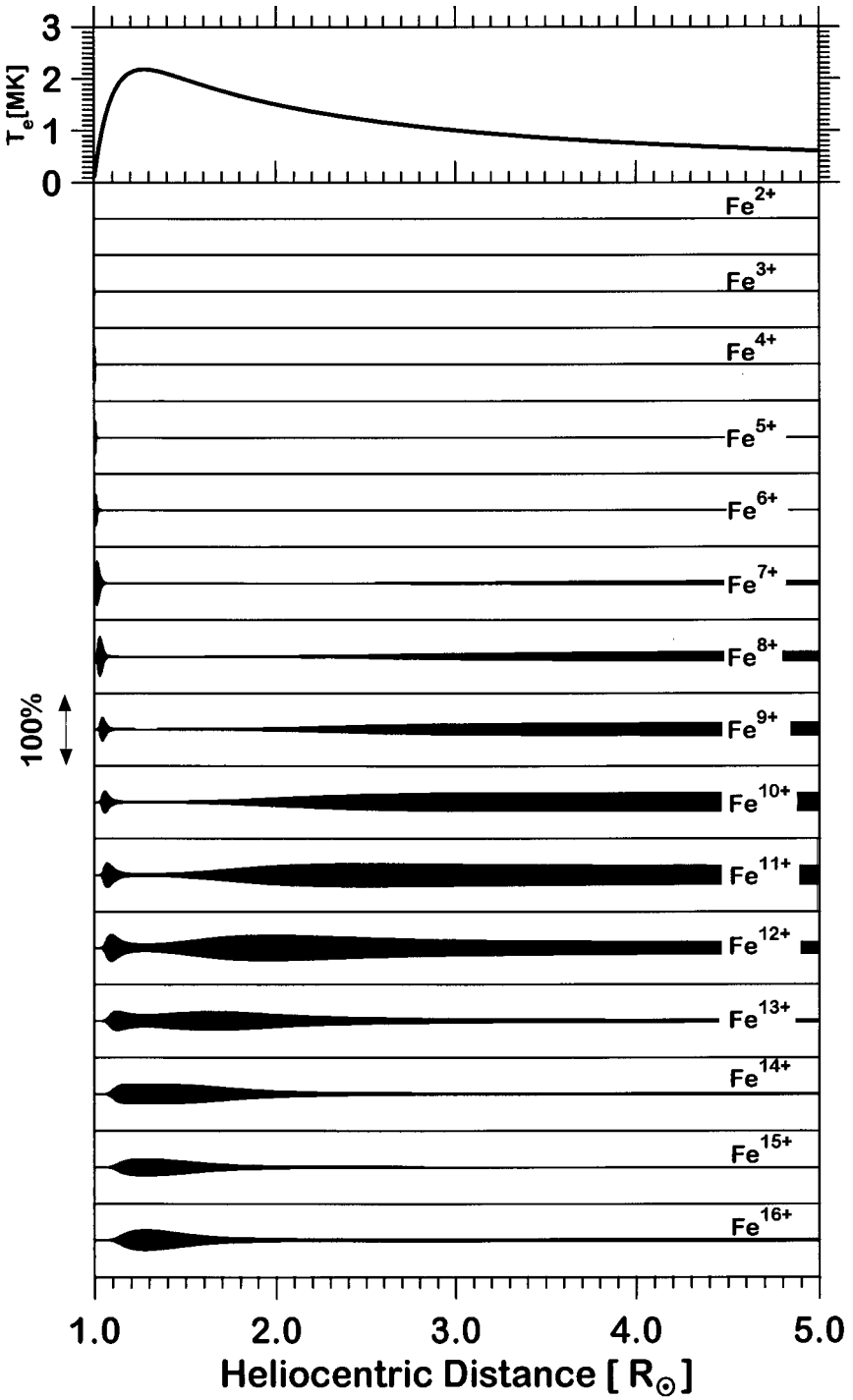

Figure 9. Result of a model on the evolution of iron charge states for the same coronal profiles as used for Figure 8. Comparison with Figure 8, which illustrates the case of oxygen, shows that the iron charge state distribution is frozen farther out in the corona. Whereas Fe^{15+} and Fe^{16+} are the dominant species at temperature maximum, recombination still proceeds rapidly enough to produce $Fe^{10+\cdots 12+}$ as the final dominant ions.

At this point some difficulties should not remain secret: Comparing freeze-in temperatures with electron temperatures, for example, line ratio temperatures derived from optical observations, gives consistent results for equatorial coronal streamers. However, in coronal hole–associated solar wind, the freeze-in temperatures often exceed those typically derived from optical observations (see *Mason and Bochsler* [1999] for a compilation of results presented at the recent SOHO7 workshop). This discrepancy is possibly due to the presence of a suprathermal tail in the electron energy distributions.

The frequently used tables of *Arnaud and Rothenflug*

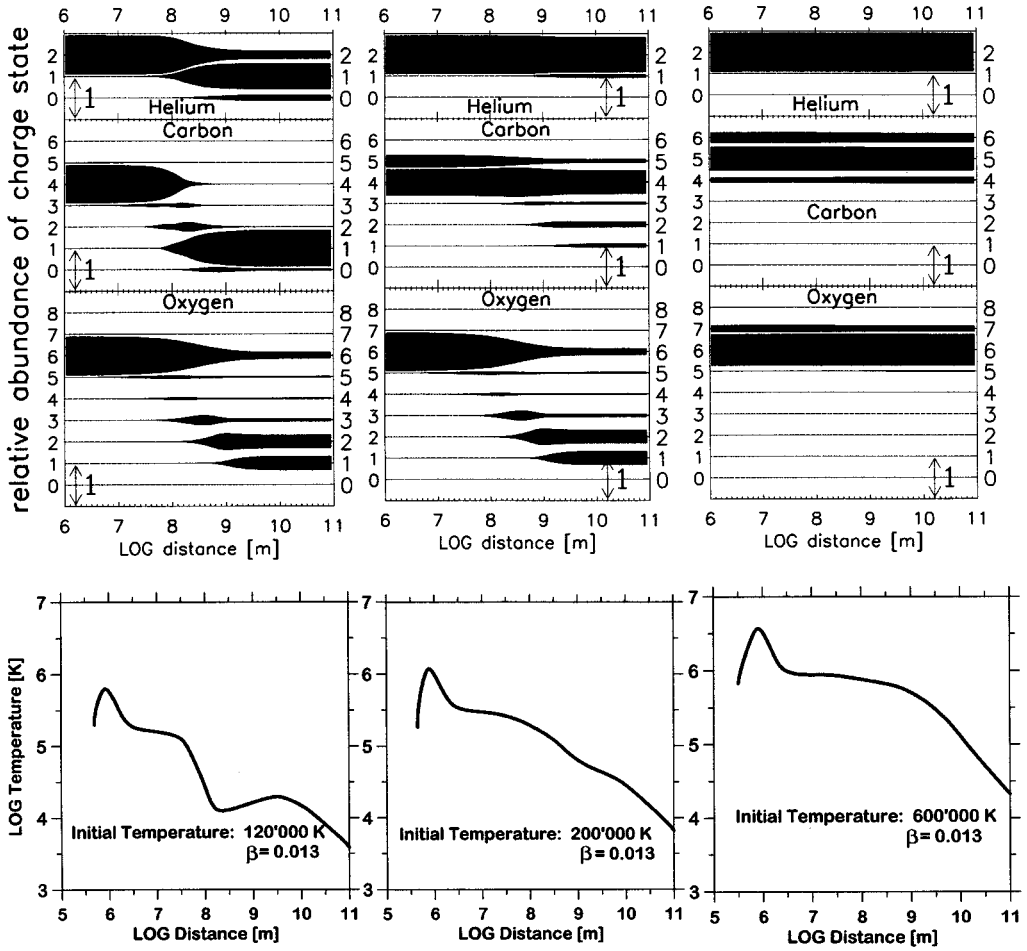

Figure 10. Numerical simulation of charge state distributions of minor ions in rapidly expanding plasmoids. In the leftmost panels the case is shown where early rapid expansion leads to freezing of anomalously low charge state such as He^{+}, C^{+}, and O^{+}. In the center panels, freezing occurs at a somewhat higher altitude from the solar surface, producing an exotic combination of He^{++}, He^{+}, C^{4+}, O^{6+}, O^{++}, and O^{+}. In the case shown in the rightmost panels the end product is indistinguishable from normal solar wind. Reprinted from *Neukomm and Bochsler* [1996] with kind permission from the American Astronomical Society.

[1985] are computed for one-parameter (i.e., Maxwellian) temperature distributions. The existence of suprathermal tails has a strong influence on ions with high ionization potential [cf. *Owocki et al.*, 1983; *Aellig et al.*, 1998]; consequently, strong deviations from charge state distributions produced with Maxwellian electrons can occur for such species.

The ionization and recombination rates sometimes differ by orders of magnitude for different species and different elements at a given temperature. For instance, at 1.6×10^6 K, O^{6+} recombines at a rate of 10^{-12} cm^3 s^{-1}, whereas the bigger ion Fe^{10+} recombines at 10^{-10} cm^3 s^{-1}. Consequently, iron charge states freeze at considerably larger distances than oxygen charge states. This property has been used to infer coronal temperature gradients [e.g., *Bame et al.*, 1974; *Aellig et al.*, 1997b]. The examples shown in Figures 8 and 9 illustrate the diversity of freeze properties. The most abundant oxygen ions (O^{6+} and O^{7+}) indicate an electron freeze-in temperature of 1.83×10^6 K. For the most abundant charge states of Ne, this reading is 1.20×10^6 K, for Na it is 1.35×10^6 K, for Mg it is 1.50×10^6 K, and for Al it is 1.65×10^6 K. The important iron species, Fe^{7+}, freezes last at only 5 $R_\odot$ at a temperature of 600,000 K. Carbon (C^{6+}/C^{5+}) freezes at 1.68×10^6 K, but at a considerably lower altitude than all the other species, i.e., before the coronal temperature maximum.

Sometimes exotic combinations of charge states are observed in conjunction with coronal mass ejections [*Schwenn et al.*, 1980; *Gosling et al.*, 1980; *Gloeckler et al.*, 1999]. For instance, *Schwenn et al.* [1980] and *Gosling et al.* [1980] found strong enhancements of He^{+} relative to normal solar wind together with O^{6+} in coronal mass ejecta. *Gloeckler et al.* [1999] also found very unusual combinations of charge states, including He^{+}, C^{2+}, and O^{3+} together with normally observed O^{6+} and O^{7+} in the May 2–3 event of 1998. The interpretation of such events is difficult. The important ingredient in explaining such observations is the fact that even if a strange combination of charge states could be created at the

origin of the coronal mass ejection (CME), for example, in the erupting filament, the plasma must cross the corona and its 10^6 K electrons at speeds not too far from normal solar wind speeds. There is no a priori reason why unusual charge states, even if created somewhere near the solar surface, should still be detectable outside the coronal temperature maximum. Hence a protecting magnetic bubble seems to be required to prevent erasure of the charge state information. Using a plasmoid model similar to the one developed by *Cargill and Pneuman* [1984], *Neukomm and Bochsler* [1996] predicted such unusual combinations as those shown in Figure 10 just for situations involving magnetic bubbles. They found that the relevant feature of these models was to include a phase of rapid, quasi-adiabatic expansion of plasmoids when the electron densities were still sufficiently large to allow recombination. In a situation where the expansion time was short compared with the recombination times, for example, of the order of less than an hour or so, the sequence of recombination is interrupted before it reaches equilibrium, with the result that low and high charge states freeze and coexist in the outflowing CME-associated solar wind.

Among the minor ions, oxygen and iron are the more abundant ones. As was discussed before, they exhibit a wide variety of ionic features, which are, however, well established at a few solar radii from the Sun. Observation of these charge states provides an important means to obtain information on physical conditions in the inner corona. Another interesting aspect is that with high time resolution observations (e.g., with SOHO/CELIAS), it has been possible to locate short (5-min) and steep transitions (see *Aellig et al*. [1997a] for a detailed discussion). Such sharp discontinuities can only be established in the inner corona, and it is amazing that they survive the journey through the turbulent interplanetary medium without being erased on their way from the corona to the site of observation at 1 AU.

6. CONCLUSIONS

At the time this paper was written, the most important concern was the consistency between coronal abundance determinations with optical methods and solar wind abundance measurements from in situ particle observations. Since the establishment of the space-based observatories SOHO and Yokoh, optical observations have greatly improved in spatial resolution, and abundance maps with a rich variety of detail have been provided. At the same time, in situ observations have been significantly enhanced in time resolution. Whereas the derivation of data from optical observations is often rendered difficult due to line-of-sight effects, in situ abundance determinations are frequently hampered by complicated instrument functions, and a sometimes insurmountable difficulty is the unraveling of flux tubes and identification of source regions in the solar atmosphere with sufficient precision. In the pre-SOHO era it was mostly rather simple to relate optical and in situ measurements given the poor temporal and spatial resolution. Connecting the pieces of the nowadays much more complicated jigsaw puzzle has become a new challenge. Nevertheless, it is a prerequisite for progress in understanding the processes which shape the solar wind composition.

ACKNOWLEDGMENTS. The author acknowledges fruitful discussions with many individuals from the Ulysses/SWICS and SOHO/CELIAS team, most important those with F. M. Ipavich, M. A. Coplan, S. A. Lasley, J. M. Paquette, M. R. Aellig, R. Neukomm, R. von Steiger, P. Wurz, and R. F. Wimmer-Schweingruber. This work was partially supported by the Swiss National Science Foundation. The author benefitted from the hospitality of F. M. Ipavich and the Space Physics Group at the University of Maryland, which made the writing of this review possible. Peter Cargill, Sylvain Turcotte, and two anonymous referees contributed many helpful comments to improve the manuscript and eliminate errors.

James Horwitz was the Editor responsible for this paper. He acknowledges Peter Cargill, Sylvain Turcotte, and one anonymous reviewer for their technical reviews and Bridget Scanlon for the cross-disciplinary review.

REFERENCES

Aellig, M. R., H. Grünwaldt, P. Bochsler, S. Hefti, R. Kallenbach, F. M. Ipavich, D. Hovestadt, M. Hilchenbach, and the CELIAS team, Solar wind iron charge states observed with high time resolution with CELIAS/CTOF, in *Proceedings of the Fifth SOHO Workshop*: *The Corona and Solar Wind Near Minimum Activity*, *Eur. Space Agency Spec. Publ. ESA SP-404*, 157–161, 1997a.

Aellig, M. R., H. Grünwaldt, P. Bochsler, S. Hefti, P. Wurz, R. Kallenbach, F. M. Ipavich, D. Hovestadt, M. Hilchenbach, and the CELIAS team, Solar wind minor ion charge states observed with high time resolution with SOHO/-CELIAS/CTOF, in *Proceedings of the 31st ESLAB Symposium*: *Correlated Phenomena at the Sun, in the Heliosphere and in Geospace*, *Eur. Space Agency Spec. Publ. ESA SP-415*, 27–31, 1997b.

Aellig, M. R., P. Bochsler, H. Grünwaldt, S. Hefti, P. Wurz, M. Hilchenbach, D. Hovestadt, F. M. Ipavich, and F. Gliem, The influence of suprathermal electrons on the derivation of coronal electron temperatures from solar wind minor ion charge states, *Phys. Chem. Earth*, *24*, 407–414, 1998.

Aellig, M. R., H. Holweger, P. Bochsler, P. Wurz, H. Grünwaldt, S. Hefti, F. M. Ipavich, and B. Klecker, The Fe/O elemental abundance ratio in the solar wind, in *Solar Wind Nine*, edited by S. R. Habbal et al., pp. 255–258, Am. Inst. of Phys., College Park, Md., 1999.

Anders, E., and N. Grevesse, Abundances of the elements: Meteoritic and solar, *Geochim. Cosmochim. Acta*, *53*, 197–214, 1989.

Arnaud, M., and R. Raymond, Iron ionization and recombination rates and ionization equilibrium, *Astrophys. J.*, *398*, 394–406, 1992.

Arnaud, M., and R. Rothenflug, An updated evaluation of recombination and ionization rates, *Astron. Astrophys. Suppl. Ser.*, *60*, 425–457, 1985.

Bame, S. J., J. R. Asbridge, W. C. Feldman, and P. D. Kearney, The quiet corona: Temperature and temperature gradient, *Sol. Phys*., *35*, 137–152, 1974.

Blöcker, T., H. Holweger, B. Freytag, F. Herwig, H.-G. Ludwig, and M. Steffen, Lithium depletion in the Sun: A study of mixing based on hydrodynamical simulations, in *Solar Composition and Its Evolution—From Core to Corona*, edited by C. Fröhlich et al., pp. 105–112, Kluwer Acad., Norwell, Mass., 1998.

Bochsler, P., Velocity and abundance of silicon ions in the solar wind, *J. Geophys. Res*., *94*, 2365–2373, 1989.

Bochsler, P., and R. Kallenbach, Fractionation of nitrogen isotopes in solar energetic particles, *Meteoritics*, *29*, 653–658, 1994.

Bodmer, R., and P. Bochsler, Fractionation of minor ions in the solar wind accelerations process, *Phys. Chem. Earth*, *23*, 687–692, 1998.

Borrini, G., J. T. Gosling, S. J. Bame, W. C. Feldman, and J. M. Wilcox, Solar wind helium and hydrogen structure near the heliospheric current sheet: A signal of coronal streamers at 1 AU, *J. Geophys. Res*., *86*, 4565–4573, 1981.

Breneman, H. H., and E. C. Stone, Solar coronal and photospheric abundances from solar energetic particle measurements, *Astrophys. J*., *299*, L57–L61, 1985.

Bürgi, A., Dynamics of alpha particles in coronal streamer type geometries, in *Solar Wind Seven*, edited by E. Marsch and R. Schwenn, pp. 333–336, Pergamon, Tarrytown, N. Y., 1992.

Cargill, P. J., and G. W. Pneuman, Diamagnetic propulsion and energy balance of magnetic elements in the solar chromospheric and transition region, *Astrophys. J*., *276*, 369–378, 1984.

Carlsson, M., and R. F. Stein, Does a nonmagnetic solar chromosphere exist?, *Astrophys. J*., *440*, L29–L32, 1995.

Cassen, P., Models for the fractionation of moderately volatile elements in the solar nebula, *Meteorit. Planet. Sci*., *31*, 793–806, 1996.

Clayton, R. N., Oxygen isotopes in meteorites, *Annu. Rev. Earth Planet. Sci*., *21*, 115–149, 1993.

Cranmer, S. R., G. B. Field, and J. L. Kohl, Spectroscopic constraints on models of ion cyclotron resonance heating in the polar solar corona and high-speed solar wind, *Astrophys. J*., *518*, 937–947, 1999.

Fisk, L. A., ^{3}He-rich flares: A possible explanation, *Astrophys. J*., *224*, 1048–1055, 1978.

Fröhlich, C., C. M. E. Huber, S. E. Solanki, and R. von Steiger (Ed.), *Solar Composition and Its Evolution—From Core to Corona*, Kluwer Acad., Norwell, Mass., 1998.

Garrard, T. L., and E. C. Stone, Composition of energetic particles from solar flares, *Adv. Space Res*., *14*(10), 589–598, 1994.

Geiss, J., Constraints on the FIP mechanisms from solar wind abundance data, in *Solar Composition and Its Evolution—From Core to Corona*, edited by C. Fröhlich et al., pp. 241–252, Kluwer Acad., Norwell, Mass., 1998.

Geiss, J., and P. Bochsler, Ion composition in the solar wind in relation to solar abundances, in *Rapports Isotopiques Dans le Système Solaire*, pp. 213–228, Cépaduès, Paris, 1985.

Geiss, J., P. Hirt, and H. Leutwyler, On acceleration and motion of ions in corona and solar wind, *Sol. Phys*., *12*, 458–483, 1970.

Geiss, J., G. Gloeckler, and R. von Steiger, Origin of the solar wind from composition data, *Space Sci. Rev*., *72*, 49–60, 1995.

Gloeckler, G., L. A. Fisk, S. Hefti, N. A. Schwadron, T. H. Zurbuchen, F. M. Ipavich, J. Geiss, P. Bochsler, and R. F. Wimmer-Schweingruber, Unusual composition of the solar wind in the May 2–3, 1998, CME observed with SWICS on ACE, *Geophys. Res. Lett*., *26*, 157–160, 1999.

Gosling, J. T., J. R. Asbridge, S. J. Bame, W. C. Feldman, and R. D. Zwickl, Observations of large fluxes of He^+ in the solar wind following an interplanetary shock, *J. Geophys. Res*., *85*, 3431–3434, 1980.

Grevesse, N., and A. J. Sauval, Standard solar composition, in *Solar Composition and Its Evolution—From Core to Corona*, edited by C. Fröhlich et al., pp. 161–174, Kluwer Acad., Norwell, Mass., 1998.

Hefti, S., et al., Kinetic properties of solar wind minor ions and protons measured with SOHO/CELIAS, *J. Geophys. Res*., *103*, 29,697–29,704, 1998.

Hénoux, J.-C., FIP fractionation: Theory, in *Solar Composition and Its Evolution—From Core to Corona*, edited by C. Fröhlich et al., pp. 215–226, Kluwer Acad., Norwell, Mass., 1998.

Ho, G. C., D. C. Hamilton, G. Gloeckler, and P. Bochsler, Enhanced solar wind $^3He^{2+}$ associated with coronal mass ejections, *Geophys. Res. Lett*., *27*, 309–312, 2000.

Hovestadt, D., et al., CELIAS—Charge, element and isotope analysis system for SOHO, *Sol. Phys*., *162*, 441–481, 1995.

Humayun, M., and R. N. Clayton, Potassium isotope cosmochemistry: Genetic implications of volatile element depletion, *Geochim. Cosmochim. Acta*, *59*, 2131–2148, 1995.

Hundhausen, A. J., H. E. Gilbert, and S. J. Bames, Ionization state of the interplanetary plasma, *J. Geophys. Res*., *73*, 5485–5493, 1968.

Ipavich, F. M., P. Bochsler, S. E. Lasley, J. M. Paquette, and P. Wurz, The abundance of sodium in the solar wind as measured by SOHO/CELIAS/MTOF (abstract), *Eos Trans. AGU*, *80*(17), Spring Meet Suppl., S256, 1999.

Isenberg, P. A., and J. V. Hollweg, On the preferential acceleration and heating of solar wind heavy ions, *J. Geophys. Res*., *88*, 3923–3935, 1983.

Judge, P. G., and H. Peter, The structure of the chromosphere, in *Solar Composition and Its Evolution—From Core to Corona*, edited by C. Fröhlich et al., pp. 187–202, Kluwer Acad., Norwell, Mass., 1998.

Kallenbach, R., et al., Isotopic composition of solar wind neon measured by CELIAS/MTOF on board SOHO, *J. Geophys. Res*., *102*, 26,895–26,904, 1997.

Kohl, J. L., et al., UVCS/SOHO empirical determinations of anisotropic velocity distributions in the solar corona, *Astrophys. J. Lett*., *501*, L127–L131, 1998.

Laughlin, G., and F. C. Adams, Possible stellar metallicity enhancements from the accretion of planets, *Astrophys. J*., *491*, L51–L54, 1997.

Marsch, E., R. von Steiger, and P. Bochsler, Element fractionation by diffusion in the solar chromosphere, *Astron. Astrophys*., *301*, 261–276, 1995.

Mason, G. M., J. E. Mazur, and D. C. Hamilton, Heavy-ion isotopic anomalies in ^{3}He-rich solar particle events, *Astrophys. J*., *425*, 843–848, 1994.

Mason, H., and P. Bochsler, Composition and elemental abundance variations in the solar atmosphere and solar wind, in *Coronal Holes and Solar Wind Acceleration*: *Proceedings of the SOHO 7 Workshop*, edited by J. L. Kohl and S. R. Cranmer, pp. 105–121, Kluwer Acad., Norwell, Mass., 1999.

Michaud, G., and S. Vauclair, Element separation by atomic diffusion, in *Solar Interior and Atmosphere*, edited by A. N. Cox, W. C. Livingston, and M. S. Matthews, pp. 304–325, Univ. of Ariz. Press, Tucson, 1991.

Neukomm, R. O., and P. Bochsler, Diagnostics of closed magnetic structures in the solar corona using charge states of helium and of minor ions, *Astrophys. J*., *465*, 462–472, 1996.

Owocki, S. P., T. E. Holzer, and A. J. Hundhausen, The solar wind ionization state as a coronal temperature diagnostic, *Astrophys. J*., *275*, 354–366, 1983.

Parker, E. N., Dynamics of the interplanetary gas and magnetic fields, *Astrophys. J*., *128*, 664–676, 1958.

Peter, H., Velocity-dependent fractionation in the solar chromosphere, *Astron. Astrophys*., *312*, L37–L40, 1996.

Reames, D. V., Solar energetic particles: Sampling coronal abundances, *Space Sci. Rev*., *85*, 327–340, 1998.

Riyopoulos, S., Subthreshold stochastic diffusion with application to selective acceleration of ^{3}He in solar flares, *Astrophys. J*., *381*, 578–582, 1991.

Schmid, J., P. Bochsler, and J. Geiss, Velocity of iron ions in the solar wind, *J. Geophys. Res*., *92*, 9901–9906, 1987.

Schwadron, N. A., L. A. Fisk, and T. H. Zurbuchen, Elemental fractionation in the slow solar wind, *Astrophys. J*., *521*, 859–867, 1999.

Schwenn, R., H. Rosenbauer, and K.-H. Mühlhäuser, Singly-ionized helium in the driver gas of an interplanetary shock wave, *Geophys. Res. Lett*., *7*, 201–204, 1980.

Tagger, M., E. Falgarone, and A. Shukurov, Ambipolar filamentation of turbulent magnetic fields, *Astron. Astrophys*., *299*, 940–946, 1995.

Temerin, M., and I. Roth, The production of ^{3}He and heavy ion enrichments in ^{3}He-rich flares by electromagnetic hydrogen cyclotron waves, *Astrophys. J. Lett*., *391*, L105–L108, 1992.

Tu, C.-Y., E. Marsch, K. Wilhelm, and W. Curdt, Ion temperatures in a solar polar coronal hole observed by SUMER on SOHO, *Astrophys. J*., *503*, 475–482, 1998.

Turcotte, S., J. Richer, G. Michaud, C. A. Iglesias, and F. J. Rogers, Consistent solar evolution model including diffusion and radiative acceleration effects, *Astrophys. J*., *504*, 539–558, 1998.

Vauclair, S., and J.-P. Meyer, Diffusion in the chromosphere and the composition of the solar corona and energetic particles, *Proc. Int. Conf. Cosmic Rays 19*, *4*, 233–236, 1985.

von Steiger, R., and J. Geiss, Supply of fractionated gases to the corona, *Astron. Astrophys*., *225*, 222–238, 1989.

Wiens, R. C., G. R. Huss, and D. S. Burnett, The solar oxygen isotopic composition: Predictions, and implications for solar nebula processes, *Meteorit. Planet. Sci*., *34*, 99–107, 1999.

Williams, D. L., R. A. Leske, R. A. Mewaldt, and E. C. Stone, Solar energetic particle isotopic composition, *Space Sci. Rev*., *85*, 379–386, 1998.

Wimmer-Schweingruber, R. F., P. Bochsler, O. Kern, G. Gloeckler, and D. C. Hamilton, First determination of the silicon isotopic composition of the solar wind: WIND/MASS results, *J. Geophys. Res*., *103*, 20,621–20,630, 1998.

Wimmer-Schweingruber, R. F., P. Bochsler, G. Gloeckler, F. M. Ipavich, J. Geiss, R. Kallenbach, L. A. Fisk, S. Hefti, and T. H. Zurbuchen, On the bulk isotopic composition of magnesium and silicon during the May 1998 CME: ACE/SWIMS, *Geophys. Res. Lett*., *26*, 165–168, 1999.

Wood, J. A., Meteoritic evidence for the infall of large interstellar dust aggregates during the formation of the solar system, *Astrophys. J*., *503*, L101–L104, 1998.

Zurbuchen, T. H., L. A. Fisk, G. Gloeckler, and N. A. Schwadron, Element and isotopic fractionation in closed magnetic structures, in *Solar Composition and Its Evolution—From Core to Corona*, edited by C. Fröhlich et al., pp. 397–406, Kluwer Acad., Norwell, Mass., 1998.

P. Bochsler, Physikalisches Institut, University of Bern, Sidlerstrasse 5, CH 3012 Bern, Switzerland. (bochsler@soho.unibe.ch)